

# Volatility-of-Volatility Risk

## Online Appendix

Darien Huang    Christian Schlag    Ivan Shaliastovich    Julian Thimme

This online appendix supplements the paper *Volatility-of-Volatility Risk* with additional information on and conclusions from a model calibration exercise (Section I), technical details about delta-hedged equity options and risk-neutral skewness (Section II), and an additional robustness check (Section III).

### I. Model

Unlike the expected gains for index options in Equation (2.10), the expected gains for VIX options do not generally admit a linear factor structure because the option price is no longer homogeneous in the underlying asset value. In this section we provide a numerical example to investigate the patterns in delta-hedged VIX option gains and how they are related to the volatility of volatility. In Section I.A, we explain how we calibrate the model. In Section I.B, we study model-implied expected gains on delta-hedged VIX options and the relation to the volatility of volatility. In Section I.C, we study the deltas of VIX options and compare them to Black-Scholes deltas.

## A. Calibration

We calibrate the model to match key asset-pricing moments in the data. The  $\mathbb{Q}$ -dynamics of the model are given in Equations (2.2) and (2.9). As it is common in the literature we choose  $\theta(V_t) = \kappa_V(\bar{V} - V_t)$  and  $\gamma(\eta_t) = \kappa_\eta(\bar{\eta} - \eta_t)$ . For simplicity, we assume that the three Brownian motions  $W^1$ ,  $W^2$  and  $W^3$  are uncorrelated.

We choose parameter values for  $r_f$ ,  $\kappa_V$ ,  $\bar{V}$ ,  $\lambda_V$ ,  $\kappa_\eta$ ,  $\bar{\eta}$ ,  $\lambda_\eta$ , and  $\phi$ . The parameters can be found in Table 1. We choose  $r_f$  and  $\bar{V}$  to match the unconditional level of risk-free rate and the variance of the S&P500 index in our sample period, respectively. We choose  $\lambda_V$ ,  $\bar{\eta}$ , and  $\kappa_V$  to target the level, the variance, and the persistence of  $VIX^2$ , respectively. These moments can be computed in closed form, because  $VIX^2$  is linear in the state variables. More specifically, it is given by

$$(1) \quad VIX_t^2 = A + B V_t$$

where the coefficients  $A$  and  $B$  are

$$(2) \quad A = \frac{\kappa_V \bar{V}}{\kappa_V + \lambda^V} \left[ 1 - \frac{1 - e^{-(\kappa_V + \lambda^V)\tau}}{(\kappa_V + \lambda^V)\tau} \right], \quad B = \frac{1 - e^{-(\kappa_V + \lambda^V)\tau}}{(\kappa_V + \lambda^V)\tau}$$

Finally, we calibrate  $\lambda_\eta$ ,  $\phi$ , and  $\kappa_\eta$  to match the level, the variance, and the persistence of  $VVIX^2$ . We run a simulation study to compute model-implied moments of  $VVIX^2$ , since they are not available in closed form. We consider a grid of states  $(V_t, \eta_t)$ , where the grid spans values between 0 and 3 times the steady state of both variables. The grid points serve as starting values for  $N$  paths of the state variables that we draw according to a discretized version of the dynamics in Equation (2.2). In particular, since  $\eta_t$  follows a square-root

process, we draw  $\eta_{t+1}$  given  $\eta_t$  from a non-central  $\chi^2$ -distribution

$$(3) \quad \eta_{t+\Delta t}^n = \frac{(1 - e^{-(\kappa_\eta + \lambda_\eta)\Delta t})\phi^2}{4(\kappa_\eta + \lambda_\eta)} \chi_d^2 \left( \frac{4\kappa_\eta e^{-\kappa_\eta\Delta t}}{(1 - e^{-(\kappa_\eta + \lambda_\eta)\Delta t})\phi^2} \eta_t^n \right) (\omega_{\eta,t+\Delta t}^n)$$

for each  $n = 1, \dots, N$ , with  $d$  degrees of freedom where

$$(4) \quad d = \frac{4\kappa_V}{\phi^2} \frac{\kappa_\eta + \lambda_\eta}{\kappa_V + \lambda_V} \bar{\eta}.$$

The increments in  $V$  are approximately Gaussian with

$$(5) \quad V_{t+\Delta t}^n = \mathcal{N} \left( V_t^n + [\kappa_V \bar{V} - (\kappa_V + \lambda^V) V_t^n] \Delta t, \Delta t \eta_t^n \right) (\omega_{V,t+\Delta t}^n).$$

To ensure non-negative realizations of the variance, we truncate the normal distribution at zero. To make the simulation results more reliable in small samples  $N$ , we use the same pseudo random numbers  $(\omega_{\eta,t+\Delta t}^n, \omega_{V,t+\Delta t}^n)$  for each grid point.

We calculate the prices of VIX futures that mature in  $t + \tau_F$ . We assume a time to maturity  $\tau_F$  of one month and choose  $\Delta t = \frac{\tau_F}{30}$ . For a given parameterization and a particular vector of initial state variables  $(V_t, \eta_t)$ , we simulate the distribution of  $V_{t+\tau_F}$  and  $\eta_{t+\tau_F}$ . We then calculate the time  $t$  futures price by

$$(6) \quad F_t(V_t, \eta_t, \tau_F) = \frac{1}{N} \sum_{n=1}^N \sqrt{A + B V_{t+\tau_F}^n}$$

The next step is calculate a grid of prices of VIX options that also mature in one month. These options are written on VIX futures that have a time to maturity of one month at the maturity of the option. To do so, we simulate state variables under  $\mathbb{Q}$  as described above and calculate the VIX futures prices at maturity of the option using the grid of futures prices calculated earlier. Since the terminal values of the drawn state variables are between the points of the futures prices grid, we interpolate (or extrapolate if a state variable is outside

the grid) the futures prices. The resulting futures price of the  $n$ -th path given initial values of  $(V_t, \eta_t)$  is denoted by  $F_{t+\tau_C}^n(V_t, \eta_t, \tau_F)$ . The call and put prices are

$$(7) \quad \begin{aligned} C_t^*(V_t, \eta_t, \tau_C, K) &= \frac{1}{N} e^{-r_f \tau_C} \sum_{n=1}^N (F_{t+\tau_C}^n(V_{t+\tau_C}, \eta_{t+\tau_C}, \tau_F) - K)^+, \\ P_t^*(V_t, \eta_t, \tau_C, K) &= \frac{1}{N} e^{-r_f \tau_C} \sum_{n=1}^N (K - F_{t+\tau_C}^n(V_{t+\tau_C}, \eta_{t+\tau_C}, \tau_F))^+ \end{aligned}$$

where  $K$  denotes the strike price. We use a grid of strike prices that ranges across values between  $0.4\bar{K}$  and  $1.6\bar{K}$ , where  $\bar{K}$  is the steady state futures price  $F_t(\bar{V}, \bar{\eta}, \tau_C + \tau_F)$ .

To calculate  $VVIX^2$ , we use VIX option prices calculated above and proceed similarly to the procedure that is applied to data. We numerically solve the integral

$$(8) \quad \begin{aligned} VVIX_t^2(V_t, \eta_t) &= \frac{2e^{r_f \tau_C}}{\tau_C} \left[ \int_0^{F_t(V_t, \eta_t, \tau_C + \tau_F)} \frac{1}{K^2} P_t^*(V_t, \eta_t, \tau_C, K) dK \right. \\ &\quad \left. \dots + \int_{F_t(V_t, \eta_t, \tau_C + \tau_F)}^\infty \frac{1}{K^2} C_t^*(V_t, \eta_t, \tau_C, K) dK \right] \end{aligned}$$

using our grid of strike prices as discretization. Futures prices  $F_t(\cdot, \cdot, \tau_C + \tau_F)$  with longer maturity are calculated as described above.

Finally, we draw one long path of the state variables under  $\mathbb{P}$ . For that purpose, we proceed as described above but use the  $\mathbb{P}$ -dynamics of the state variables:

$$(9) \quad \eta_{t+\Delta t} = \frac{(1 - e^{-\kappa_\eta \Delta t})\phi^2}{4\kappa_\eta} \chi_d^2 \left( \frac{4\kappa_\eta e^{-\kappa_\eta \Delta t}}{(1 - e^{-\kappa_\eta \Delta t})\phi^2} \eta_t \right) (\omega_{\eta, t+\Delta t}^0),$$

with  $d$  degrees of freedom where

$$(10) \quad d = \frac{4\kappa_\eta}{\phi^2} \bar{\eta}$$

and

$$(11) \quad V_{t+\Delta t} = \mathcal{N}\left(V_t + \kappa_V(\bar{V} - V_t)\Delta t, \Delta t \eta_t\right)(\omega_{V,t+\Delta t}^0).$$

Using our grid of  $VIX$  and  $VVIX$ , we can now study the time series properties of the model-implied quantities and compare them with the empirical moments.

## B. Expected gains on delta-hedged VIX options

To calculate model-implied delta-hedged option gains, we calculate prices of VIX futures and VIX options on a grid, as described in Section I.A. We use Equation (2.18) and numerically solve the integral

$$(12) \quad \int_t^{t+\tau} \mathbb{E}_t \left[ \frac{\partial C_s^*}{\partial \eta_s} \lambda_s^\eta \right] ds.$$

We approximate the continuous path of  $\frac{\partial C_s^*}{\partial \eta_s}$  by a discretization with step size  $\Delta t$ :

$$(13) \quad \int_t^{t+\tau} \mathbb{E}_t \left[ \frac{\partial C_s^*}{\partial \eta_s} \lambda_s^\eta \right] ds \approx \frac{1}{N} \sum_{n=1}^N \sum_{i=0}^{I-1} \frac{\partial C_{t+i\Delta t}^*(V_{t+i\Delta t}^n, \eta_{t+i\Delta t}^n, \tau_C - i\Delta t, K)}{\partial \eta_{t+i\Delta t}} \lambda_{t+i\Delta t}^\eta \Delta t,$$

where  $I\Delta t = \tau$ . We implement this equation in the following way: First, we compute grids of VIX option prices according to the procedure outlined in Section I.A also for shorter times to maturity, in particular,  $\tau_C - i\Delta t$  for  $i = 0, \dots, I$ . Second, we approximate the derivative of  $C^*$  with respect to  $\eta$  using finite differences, i.e., at the grid point  $(V_{m_V}, \eta_{m_\eta})$ , we use

$$(14) \quad \frac{\partial C^*(V_{m_V}, \eta_{m_\eta})}{\partial \eta_{m_\eta}} \approx \frac{C^*(V_{m_V}, \eta_{m_\eta+1}) - C^*(V_{m_V}, \eta_{m_\eta-1})}{\eta_{m_\eta+1} - \eta_{m_\eta-1}}.$$

Third, we again simulate innovations in the state variables under  $\mathbb{P}$ . After each simulation step, we end up in states which are between two grid points or even outside the grid.

Because we do not have derivatives at these points, we proceed as follows. We start with the calculation of expected option gains over the last time step from  $t + \tau_C - \Delta t$  to  $t + \tau_C$ . This gives us a grid of expected option gains over this short period. We then simulate increments in the state variables in the period from  $t + \tau_C - 2\Delta t$  to  $t + \tau_C - \Delta t$ , starting again with the usual  $(V, \eta)$ -grid and add up expected gains over this period with expected gains over the final period given the state that is drawn using the scheme that approximates the  $\mathbb{P}$  dynamics (see Section I.A). We do so by interpolating the grid produced before. We use the same procedure and iterate back until time  $t$ .

Figure 1 shows expected delta-hedged option gains divided by the futures price as a function of  $\eta$  for different levels of the variance  $V_t$ . For the upper graph we choose  $\lambda_\eta = -5$ , i.e. we assume that the market price of volatility-of-volatility risk is negative. For the lower graph we assume  $\lambda_\eta = 5$ . For the strategies shown here, we always choose at-the-money options. When the investor sets up a strategy in state  $(V_0, \eta_0)$ , the strike price of the option he buys is equal to the VIX futures price in state  $(V_0, \eta_0)$ , i.e., to  $F_t(V_0, \eta_0, \tau_F)$ .

Given a negative  $\lambda_\eta$ , we find that the expected gains are all negative.<sup>1</sup> This is because the derivatives of the VIX options with respect to  $\eta$  are positive for all grid points and for all times to maturity. We also find that expected option gains are larger in absolute terms for higher values of  $\eta$ . Since we truncate the process for  $V$  at zero, this effect is more pronounced for low values of  $V$ : A high volatility of volatility not only increases the value of the VIX option because the option price is convex in  $V$ , but also because it increases the upside potential of the *VIX* without increasing the downside potential, due to the lower bound at zero. Expected option gains are not exactly linear in  $\eta_t$  since the derivative of VIX option prices with respect to  $\eta$  is not constant but decreasing in  $\eta$  (see Figure 2).

With a positive  $\lambda_\eta$  expected delta-hedged option gains are positive. In this case, all VIX

---

<sup>1</sup>Quantitatively, the expected delta-hedged VIX option gains normalized by the VIX futures price, computed at the average values of the volatility states, are about -0.1% for two-day returns, or -1.5% time-aggregated to a monthly horizon. These values are close to the empirical estimates presented in Section 5.

option prices are still increasing in the volatility of volatility. We can conclude that the sign of the expected option gain is pinned down by the sign of the market price of volatility of volatility risk, and that the expected delta-hedged VIX option gains are increasing, in absolute terms, in the volatility of volatility.

## C. Delta computations

A key input into the computations of delta-hedged option returns is the delta of the option. A typical approach in the literature is to approximate the unknown "true" deltas by the Black-Scholes implied ones; see Bakshi and Kapadia (2003), Duarte and Jones (2007), and our subsequent analysis. In this section, we use our numerical model to compute and compare the "true" and Black-Scholes deltas, and evaluate the adequacy of the approximation for the VIX options.

The Black-Scholes delta for a call option on a futures contract is given by  $\Delta = e^{-r_f \tau_C} N(d_1)$  where  $N$  denotes the standard normal cumulative distribution function, and  $d_1$  is given as

$$(15) \quad d_1 = \frac{\log(F_t(V, \eta)) - \log(K) + \frac{1}{2}IV^2\tau_C}{IV\sqrt{\tau_C}}.$$

Here,  $IV$  denotes the implied volatility of the underlying. We use the observed option and futures prices and solve the Black Scholes formula for  $IV$ .

The Black-Scholes model assumes that the option's underlying follows a geometric Brownian motion. In our model  $V_t$  does not follow such a process. As a consequence, neither the VIX nor VIX futures prices follow a proportional process. In particular, the variance of the VIX futures price is largely driven by  $\eta$ , while its level is largely driven by  $V$ .

To evaluate the quality of the approximation, we compute the true delta from the model,  $\frac{\partial C^*}{\partial F}$ . The two prices  $C^*$  and  $F$  are both functions of  $V$  and  $\eta$ . An innovation in  $F$  can be due

to an innovation in  $V$  or in  $\eta$ , and these two innovations may lead to different innovations in  $C^*$ . The goal is to set up a portfolio that is neutral to innovations in the variance  $V$ , such that the portfolio is in the end only exposed to innovations in the volatility of volatility. It is therefore appropriate to consider the derivative in the  $V$ -*direction* only. We use the chain rule to come up with

$$(16) \quad C_{Fv}^* = \frac{\partial C^* / \partial V}{\partial F / \partial V}$$

as a proxy for  $\frac{\partial C^*}{\partial F}$ .  $C_{Fv}^*$  quantifies how much the VIX option price changes after a change in  $F$  that is due to a change in  $V$ .

Figure 3 shows both variants of delta as functions of the state variables  $V$  and  $\eta$ . The plotted deltas are for options with a strike price of  $F(\bar{V}, \bar{\eta})$ . We find that the two variants of delta have a similar shape, but  $C_{Fv}^*$  is closer to 0 when the option is deep in the money and closer to 1 when the option is far out of the money. The Black Scholes delta of the at-the-money option is equal to 0.63 while  $C_{Fv}^*$  of the at-the-money option is 0.60. In the empirical part of our paper we use mostly at-the-money options and test if the results are robust to variations in deltas.

Instead of using Equation (2.18) to calculate expected option gains, one could alternatively simulate realized gains from the trading strategy and take the average across realizations. For this purpose, we would have to calculate deltas of the VIX options and set up a delta hedged portfolio. This procedure, however, has the disadvantage that we need much larger samples to obtain stable results, because of the fluctuations in the Brownian motion  $W_3$  that are averaged out when taking the expectation (see Equation (2.17)). While this task is very costly in terms of computation time, one can look at realized delta hedged option gains path by path and study the difference between gains when different deltas are used for setting up the hedge portfolio.

We now compare the difference between gains from our trading strategy when using the Black-Scholes delta or the “true” delta  $C_{FV}^*$  for setting up the hedge portfolio. Even with noisy estimates of the expected gains, the difference between both gains is informative because we use the same paths of the state variables in the simulation of the two strategies. Thus, the sampling error widely cancels out when considering the difference.

Figure 4 shows the difference between delta hedged option gains when using either delta. For moderate values of  $V$  the difference is close to zero. When  $V$  is high, the strategy that uses the Black-Scholes delta yields less negative returns than the strategy that uses  $C_{FV}^*$ . In the light of this result, we can conclude that using Black-Scholes deltas is a rather conservative strategy. In our empirical exercise, we would expect even more pronounced gains when using  $C_{FV}^*$ , which is, however, not observable in the data.

## II. Technical Details

### A. Delta-Hedged Equity Options

The state vector is  $x_t = \begin{bmatrix} S_t & V_t & \eta_t \end{bmatrix}'$ . Under the linear risk premium structure,  $\lambda_t^V = \lambda^V V_t$  and  $\lambda_t^\eta = \lambda^\eta \eta_t$ . Note that since  $C_t$  is homogeneous of degree 1 in the underlying  $S_t$  and the strike price  $K$ ,  $\frac{\partial C}{\partial V}$  and  $\frac{\partial C}{\partial \eta}$  are also homogeneous of degree 1 in  $S_t$  and  $K$ . Define a pair of functions:

$$(17) \quad \begin{aligned} g_1(x_t) &= \lambda_t^V \frac{\partial C_t}{\partial V_t} \\ g_2(x_t) &= \lambda_t^\eta \frac{\partial C_t}{\partial \eta_t} \end{aligned}$$

We can re-write Equation (8) from the paper as:

$$(18) \quad \mathbb{E}_t [\Pi_{t,t+\tau}] = \mathbb{E}_t \left[ \int_t^{t+\tau} g_1(x_u) du \right] + \mathbb{E}_t \left[ \int_t^{t+\tau} g_2(x_u) du \right].$$

Define operators  $\mathcal{L}$  and  $\Gamma$  such that:

$$(19) \quad \begin{aligned} \mathcal{L}[\cdot] dt &= \frac{\partial[\cdot]}{\partial S} \mu_t S_t dt + \frac{\partial[\cdot]}{\partial V} \theta(V_t) dt + \frac{\partial[\cdot]}{\partial \eta} \gamma(\eta_t) dt + \frac{\partial[\cdot]}{\partial t} dt \\ &+ \frac{1}{2} \frac{\partial^2[\cdot]}{\partial S^2} [dS_t, dS_t] + \frac{1}{2} \frac{\partial^2[\cdot]}{\partial V^2} [dV_t, dV_t] + \frac{1}{2} \frac{\partial^2[\cdot]}{\partial \eta^2} [d\eta_t, d\eta_t] \\ &+ \frac{\partial^2[\cdot]}{\partial S \partial \eta} [dS_t, d\eta_t] + \frac{\partial^2[\cdot]}{\partial S \partial V} [dS_t, dV_t] + \frac{\partial^2[\cdot]}{\partial V \partial \eta} [dV_t, d\eta_t] \\ \Gamma[\cdot] &= \left[ \frac{\partial[\cdot]}{\partial S} S_t \sqrt{V_t}, \frac{\partial[\cdot]}{\partial V} \sqrt{\eta_t}, \frac{\partial[\cdot]}{\partial \eta} \phi \sqrt{\eta_t} \right]. \end{aligned}$$

Then, for  $u > t$ , Itô's Lemma implies that:

$$(20) \quad g_1(x_u) = g_1(x_t) + \int_t^u \mathcal{L}g(x_{u'}) du' + \int_t^u \Gamma g(x_{u'}) dW_{u'}.$$

The integral in the first expectation on the right-hand side of Equation (18) becomes:

$$(21) \quad \begin{aligned} \int_t^{t+\tau} g_1(x_u) du &= \int_t^{t+\tau} \left[ g_1(x_t) + \int_t^u \mathcal{L}g(x_{u'}) du' + \int_t^u \Gamma g(x_{u'}) dW_{u'} \right] du \\ &= g_1(x_t) \tau + \frac{1}{2} \mathcal{L}g_1(x_t) \tau^2 + \frac{1}{6} \mathcal{L}^2 g_1(x_t) \tau^3 + \dots + \text{Itô Integrals} \\ &= \sum_{n=0}^{\infty} \frac{\tau^{1+n}}{(1+n)!} \mathcal{L}^n g_1(x_t) + \text{Itô Integrals}, \end{aligned}$$

and likewise for the second integral in (18). We can use this to re-write (18) as:

$$(22) \quad \begin{aligned} \mathbb{E}_t [\Pi_{t,t+\tau}] &= \mathbb{E}_t \left[ \int_t^{t+\tau} g_1(x_u) du \right] + \mathbb{E}_t \left[ \int_t^{t+\tau} g_2(x_u) du \right] \\ &= \sum_{n=0}^{\infty} \frac{\tau^{1+n}}{(1+n)!} \mathcal{L}^n [g_1(x_t)] + \sum_{n=0}^{\infty} \frac{\tau^{1+n}}{(1+n)!} \mathcal{L}^n [g_2(x_t)]. \end{aligned}$$

Note that  $g_1(x_t) = \alpha_1(V_t, \tau; K)S_t$ , and  $g_2(x_t) = \alpha_2(\eta_t, \tau; K)S_t$ . By Lemma 1 of Bakshi and Kapadia (2003),  $\mathcal{L}^n[g_1(x_t)]$  and  $\mathcal{L}^n[g_2(x_t)]$  will also be proportional to  $S_t$ , which implies that:

$$(23) \quad \begin{aligned} \mathcal{L}^n[g_1(x_t)] &= \lambda^V V_t \Phi_{t,n}^V S_t \quad \forall n \\ \mathcal{L}^n[g_2(x_t)] &= \lambda^\eta \eta_t \Phi_{t,n}^\eta S_t \quad \forall n. \end{aligned}$$

Therefore, we have:

$$(24) \quad \begin{aligned} \mathbb{E}_t[\Pi_{t,t+\tau}] &= \sum_{n=0}^{\infty} \frac{\tau^{1+n}}{(1+n)!} \mathcal{L}^n[g_1(x_t)] + \sum_{n=0}^{\infty} \frac{\tau^{1+n}}{(1+n)!} \mathcal{L}^n[g_2(x_t)] \\ &= S_t [\lambda^V \beta_t^V V_t + \lambda^\eta \beta_t^\eta \eta_t], \end{aligned}$$

which implies that:

$$(25) \quad \frac{\mathbb{E}_t[\Pi_{t,t+\tau}]}{S_t} = \lambda^V \beta_t^V V_t + \lambda^\eta \beta_t^\eta \eta_t,$$

where the sensitivities to the risk factors are given by:

$$(26) \quad \begin{aligned} \beta_t^V &= \sum_{n=0}^{\infty} \frac{\tau^{1+n}}{(1+n)!} \Phi_{t,n}^V > 0 \\ \beta_t^\eta &= \sum_{n=0}^{\infty} \frac{\tau^{1+n}}{(1+n)!} \Phi_{t,n}^\eta > 0. \end{aligned}$$

The betas are positive since  $\frac{\partial C_t}{\partial V_t} > 0$  and  $\frac{\partial C_t}{\partial \eta_t} > 0$ .

## B. Risk-Neutral Skewness

The prices of the volatility, cubic, and quartic contracts  $V_{t,t+\tau}$ ,  $W_{t,t+\tau}$ ,  $X_{t,t+\tau}$  are given

$$\begin{aligned}
(27) \quad V_{t,t+\tau} &= \int_{S_t}^{\infty} \frac{2(1 - \log \frac{K}{S_t})}{K^2} C_t(t + \tau; K) dK + \int_0^{S_t} \frac{2(1 + \log \frac{S_t}{K})}{K^2} P_t(t + \tau; K) dK, \\
W_{t,t+\tau} &= \int_{S_t}^{\infty} \frac{6 \log \frac{K}{S_t} - 3(\log \frac{K}{S_t})^2}{K^2} C_t(t + \tau; K) dK \\
&\quad - \int_0^{S_t} \frac{6 \log \frac{S_t}{K} + 3(\log \frac{S_t}{K})^2}{K^2} P_t(t + \tau; K) dK, \\
X_{t,t+\tau} &= \int_{S_t}^{\infty} \frac{12(\log \frac{K}{S_t})^2 - 4(\log \frac{K}{S_t})^3}{K^2} C_t(t + \tau; K) dK \\
&\quad + \int_0^{S_t} \frac{12(\log \frac{S_t}{K})^2 + 4(\log \frac{S_t}{K})^3}{K^2} P_t(t + \tau; K) dK,
\end{aligned}$$

$$\text{and } \mu_{t,t+\tau} = e^{rf\tau} - 1 - \frac{e^{rf\tau}}{2} V_{t,t+\tau} - \frac{e^{rf\tau}}{6} W_{t,t+\tau} - \frac{e^{rf\tau}}{24} X_{t,t+\tau}.$$

To construct these measures, we use out-of-the-money options to mitigate liquidity concerns. Following Shimko (1993), each day we interpolate the Black-Scholes implied volatility curve at the observable strikes using a cubic spline, and then calculate option prices to compute the above moments. We construct these measures for both S&P500 options and VIX options. Our implied volatility slope and risk-neutral skewness measures are calculated using options with the same maturity as our test assets.

## III. Additional Robustness

As stated in Section V.A of the paper, we considered an exercise similar to Coval and Shumway (2001) by perturbing the Black-Scholes deltas used in the option hedging. In Tables 2 and 3, we set the deltas to 0.95 and 1.05 times the value from the Black-Scholes model, respectively. Our main results are not sensitive to the choice of using Black-Scholes deltas for option hedging, and remain quite robust.

## References

- Bakshi, Gurdip, and Nikunj Kapadia, 2003, Delta-hedged gains and the negative market volatility risk premium, *Review of Financial Studies* 16, 527–566.
- Coval, Joshua, and Tyler Shumway, 2001, Expected option returns, *Journal of Finance* 56, 983–1009.
- Duarte, Jefferson, and Christopher Jones, 2007, The price of market volatility risk, Working paper.
- Shimko, David, 1993, Bounds of probability, *RISK* 6, 33–37.

## Tables and Figures

Table 1: **Model parameters**

The table shows the calibrated parameters for the model. Variance and vol-of-vol refers to the parameters of the variance and volatility-of-volatility dynamics, respectively. Times-to-maturity indicate the time intervals at annual frequency.

<b>Variance</b>	$\bar{V}$	$\kappa_V$	$\lambda_V$	
	.1979 <sup>2</sup>	2.4982	−4.8	
<b>Vol-of-vol</b>	$\bar{\eta}$	$\kappa_\eta$	$\phi$	$\lambda_\eta$
	.0329	13.097	.0694	−5
<b>Risk-free rate</b>	$r_f$			
	.0102			
<b>Times to maturity</b>	$\Delta t$	$\tau$	$\tau_F$	$\tau_C$
	1/360	2/360	30/360	10/360

Table 2: **Delta-Hedged Option Gains:  $0.95 \times \Delta_{BS}$  Delta**

The table shows average delta-hedged option gains on the S&P500 and VIX options across their moneyness, when the Black-Scholes delta is reduced to  $0.95 \times \Delta_{BS}$ . Options have one month to maturity, are grouped into an equal-weighted portfolio inside the moneyness bin, and are held till expiration. The delta-hedge is computed using the Black-Scholes formula, with daily rebalancing and the margin difference earning the risk-free rate. The delta-hedged option gains  $\Pi$  are scaled either by the index or by the option price. The t-statistics are testing the null that the delta-hedged option gain is equal to zero. The  $\% < 0$  column shows the fraction of observations with negative gains. The data are monthly from 2006m2 to 2016m12.

		$\frac{\Pi}{S}(\%)$						$\frac{\Pi}{C}(\%)$		
moneyness		mean	t-stat.	median	% < 0	std.	AR(1)	mean	t-stat.	median
Panel A: S&P500 Options										
Call	0.950 to 0.975	0.07	[ 3.63]	0.04	45%	0.51	0.36	1.70	[ 4.21]	0.81
	0.975 to 1.000	0.05	[ 3.29]	-0.01	52%	0.46	0.23	2.62	[ 4.38]	-0.30
	1.000 to 1.025	-0.03	[-2.50]	-0.05	57%	0.42	0.07	-2.08	[-1.54]	-4.97
	1.025 to 1.050	-0.08	[-6.86]	-0.05	62%	0.36	0.11	-31.52	[-8.87]	-22.31
Put	0.950 to 0.975	-0.14	[-7.24]	-0.20	83%	0.61	0.35	-20.09	[-8.85]	-31.90
	0.975 to 1.000	-0.17	[-9.01]	-0.22	77%	0.59	0.20	-11.02	[-7.68]	-20.48
	1.000 to 1.025	-0.23	[-11.36]	-0.26	75%	0.60	0.05	-9.34	[-12.36]	-13.36
	1.025 to 1.050	-0.28	[-10.16]	-0.31	74%	0.62	0.06	-6.47	[-10.75]	-7.71
Panel B: VIX Options										
Call	0.800 to 0.900	-0.38	[-2.17]	-0.83	61%	2.65	-0.05	-2.13	[-2.03]	-4.46
	0.900 to 1.000	-0.90	[-4.06]	-1.70	69%	3.26	-0.12	-7.80	[-3.94]	-14.21
	1.000 to 1.100	-0.94	[-3.65]	-1.65	73%	3.50	-0.15	-11.05	[-3.36]	-20.47
	1.100 to 1.200	-1.32	[-5.38]	-1.73	79%	3.25	-0.13	-20.90	[-5.11]	-29.08
Put	0.800 to 0.900	-0.44	[-1.51]	-0.73	63%	2.62	0.07	-11.33	[-1.44]	-23.15
	0.900 to 1.000	-0.73	[-3.52]	-1.03	70%	2.95	-0.14	-10.13	[-2.99]	-16.30
	1.000 to 1.100	-0.74	[-3.14]	-0.79	66%	3.20	-0.18	-5.48	[-2.97]	-6.53
	1.100 to 1.200	-1.05	[-4.31]	-0.86	69%	3.18	-0.12	-4.97	[-4.30]	-4.87

Table 3: **Delta-Hedged Option Gains:  $1.05 \times \Delta_{BS}$  Delta**

The table shows average delta-hedged option gains on the S&P500 and VIX options across their moneyness, when the Black-Scholes delta is increased to  $1.05 \times \Delta_{BS}$ . Options have one month to maturity, are grouped into an equal-weighted portfolio inside the moneyness bin, and are held till expiration. The delta-hedge is computed using the Black-Scholes formula, with daily rebalancing and the margin difference earning the risk-free rate. The delta-hedged option gains  $\Pi$  are scaled either by the index or by the option price. The t-statistics are testing the null that the delta-hedged option gain is equal to zero. The % < 0 column shows the fraction of observations with negative gains. The data are monthly from 2006m2 to 2016m12.

		$\frac{\Pi}{S}(\%)$						$\frac{\Pi}{C}(\%)$		
moneyness		mean	t-stat.	median	% < 0	std.	AR(1)	mean	t-stat.	median
<b>Panel A: S&amp;P500 Options</b>										
Call	0.950 to 0.975	0.07	[ 2.68]	-0.04	56%	0.64	0.29	1.51	[ 3.03]	-0.86
	0.975 to 1.000	0.04	[ 1.96]	-0.07	56%	0.57	0.13	2.15	[ 2.98]	-2.61
	1.000 to 1.025	-0.04	[-2.66]	-0.08	60%	0.48	0.10	-2.82	[-1.87]	-9.11
	1.025 to 1.050	-0.08	[-6.06]	-0.05	63%	0.40	0.14	-34.43	[-8.96]	-25.11
Put	0.950 to 0.975	-0.13	[-8.46]	-0.16	79%	0.48	0.34	-18.45	[-9.05]	-25.34
	0.975 to 1.000	-0.15	[-10.66]	-0.17	72%	0.43	0.19	-9.47	[-7.97]	-13.93
	1.000 to 1.025	-0.20	[-14.58]	-0.19	76%	0.40	0.01	-8.20	[-14.76]	-8.48
	1.025 to 1.050	-0.22	[-13.33]	-0.20	80%	0.38	0.01	-5.21	[-13.55]	-5.15
<b>Panel B: VIX Options</b>										
Call	0.800 to 0.900	-0.11	[-0.77]	-0.45	57%	2.26	0.06	-0.63	[-0.71]	-2.54
	0.900 to 1.000	-0.63	[-3.29]	-0.99	67%	2.84	-0.03	-5.73	[-3.37]	-9.49
	1.000 to 1.100	-0.75	[-3.26]	-1.04	68%	3.12	-0.16	-9.01	[-3.17]	-12.89
	1.100 to 1.200	-1.08	[-4.56]	-1.39	77%	3.14	-0.12	-17.11	[-4.38]	-21.77
Put	0.800 to 0.900	-0.56	[-1.79]	-1.19	67%	2.80	0.06	-14.20	[-1.63]	-32.17
	0.900 to 1.000	-0.87	[-3.85]	-1.60	70%	3.20	-0.13	-11.69	[-3.12]	-24.20
	1.000 to 1.100	-0.93	[-3.59]	-1.94	73%	3.51	-0.17	-6.79	[-3.28]	-13.46
	1.100 to 1.200	-1.30	[-5.18]	-1.72	79%	3.28	-0.14	-6.10	[-5.02]	-8.40

Figure 1: **Model-implied Expected Delta-hedged VIX Option Gains**

The figures show model-implied expected delta-hedged option gains as a function of the volatility-of-volatility  $\eta$  for different levels of the volatility state  $V_t$ . The upper plot shows gains for a negative market price of volatility-of-volatility risks,  $\lambda_\eta = -5$ . The lower plot shows gains for a positive market price of volatility-of-volatility risks  $\lambda_\eta = 5$ . All options are at the money.

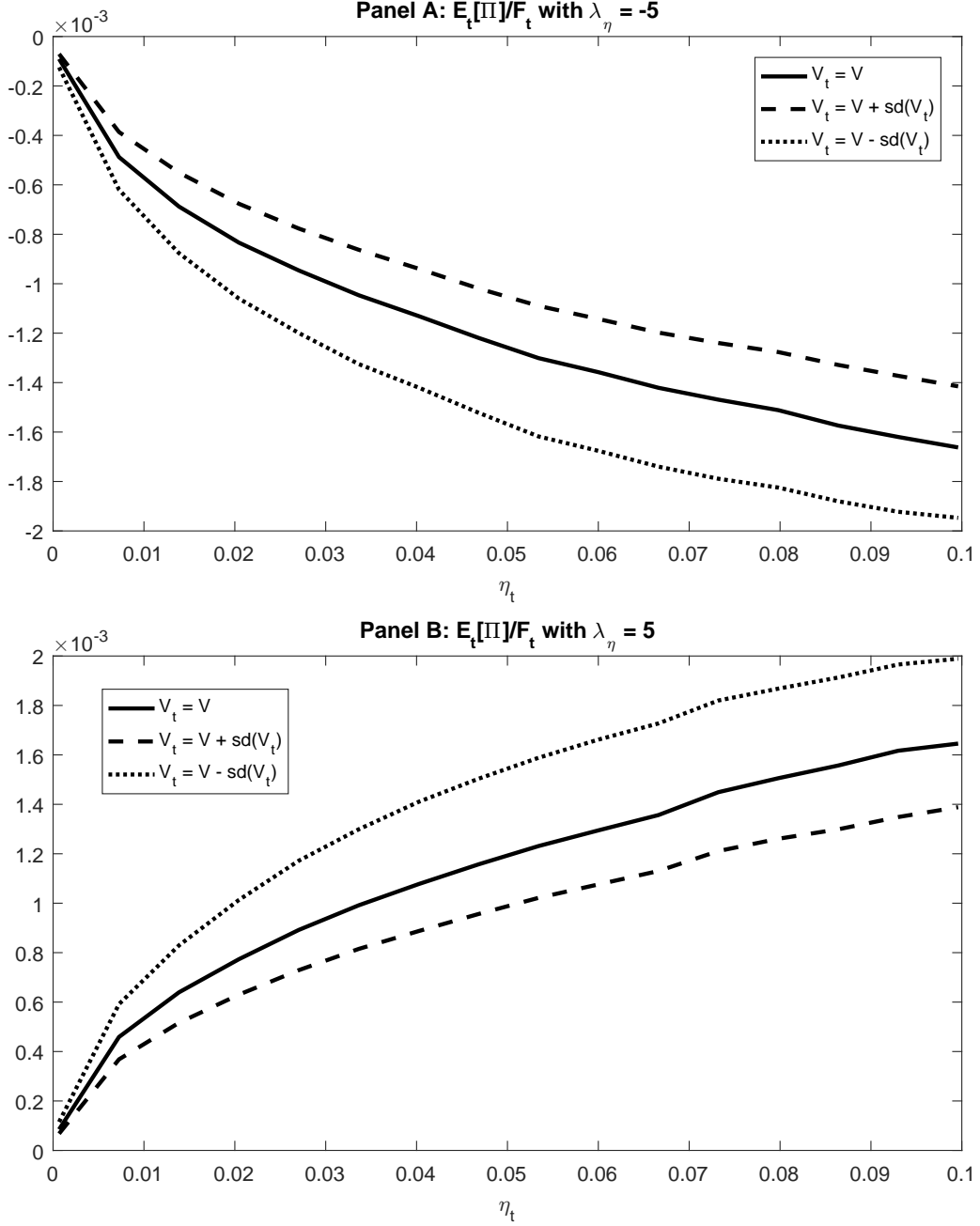


Figure 2: **Model-implied Sensitivities of VIX Option Prices**

The figure shows model-implied sensitivities (derivatives) of at-the-money VIX option prices to the volatility-of-volatility  $\eta$  as a function of the state variable  $\eta$  for different levels of  $V_t$ . The upper plot shows gains for a negative market price of volatility-of-volatility risks,  $\lambda_\eta = -5$ . The lower plot shows gains for a positive market price of volatility-of-volatility risks  $\lambda_\eta = 5$ .

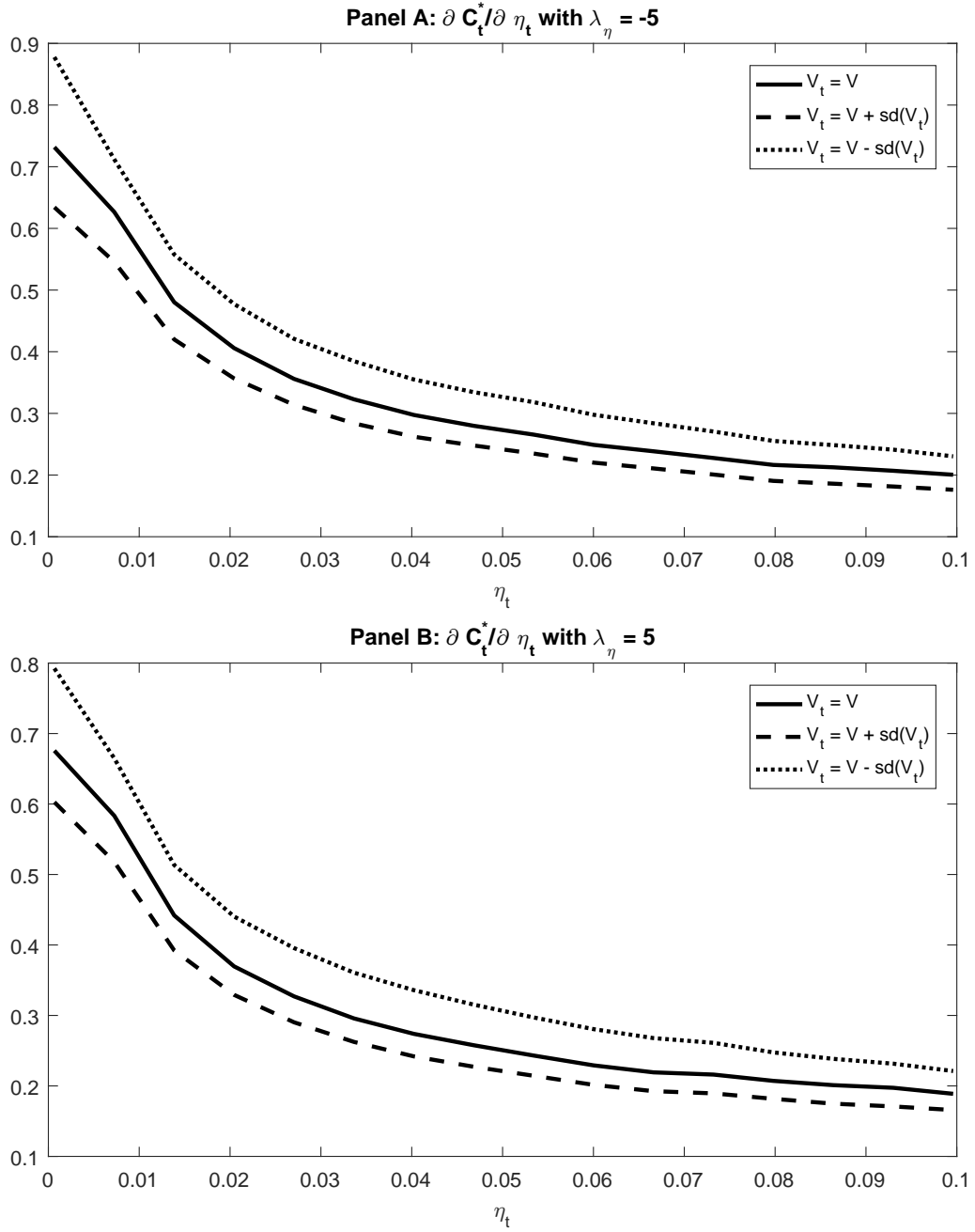


Figure 3: **Black-Scholes and Model-implied Deltas**

The figure plots the Black-Scholes delta of a VIX option (left panel) and the model-implied delta (right panel) as functions of the volatility and volatility of volatility state variables  $V$  and  $\eta$ .

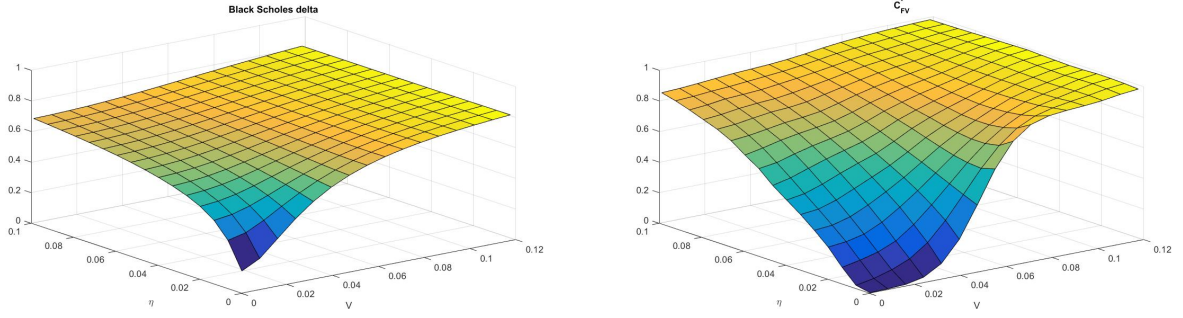


Figure 4: **Difference Between Delta-Hedged Option Gains**

The figure plots the difference between the delta-hedged option gains using the model-implied versus the Black-Scholes delta. All options are at-the-money.

